

Published in final edited form as:

Nat Biotechnol. 2010 February ; 28(2): 167–171. doi:10.1038/nbt.1604.

Real-time imaging of hepatitis C virus infection using a fluorescent cell-based reporter system

Christopher T. Jones¹, Maria Teresa Catanese¹, Lok Man J. Law¹, Salman R. Khetani^{2,5}, Andrew J. Syder^{1,6}, Alexander Ploss¹, Thomas S. Oh¹, John W. Schoggins¹, Margaret R. MacDonald¹, Sangeeta N. Bhatia^{2,3,4}, and Charles M. Rice¹

¹Center for the Study of Hepatitis C, The Rockefeller University, 1230 York Ave, New York, NY 10065

²Division of Health Sciences and Technology, Department of Electrical Engineering and Computer Science, Massachusetts Institute of Technology, 77 Massachusetts Avenue, E19-502D, Cambridge, MA 02139

³Howard Hughes Medical Institute

⁴Division of Medicine, Brigham & Women's Hospital, Boston, MA 02115

Abstract

Hepatitis C virus (HCV), which infects 2-3% of the world population, is a causative agent of chronic hepatitis and the leading indication for liver transplantation¹. The ability to propagate HCV in cell culture (HCVcc) is a relatively recent breakthrough, and a key tool in the quest for specific antiviral therapeutics. Monitoring HCV infection in culture generally involves bulk population assays and/or terminal processing of potentially precious samples. Live-cell imaging avoids this, but necessitates genetically modified reporter viruses, which often exhibit profound replication defects. Here we develop a cell-based fluorescent reporter system that allows sensitive distinction of individual HCV-infected cells in live or fixed samples. We demonstrate use of this technology for several previously intractable applications, including live-cell imaging of viral propagation and host response, as well as visualizing infection of primary hepatocyte cultures. Integration of this reporter with modern image-based analysis methods could open new doors for HCV research.

A known cellular substrate of the HCV NS3-4A protease²⁻⁴, the mitochondrially-tethered IFN- β promoter stimulator protein 1 (IPS-1⁵) - also termed MAVS⁶, VISA⁷, or Cardif² - was adapted for use as a marker of infection. The carboxy-terminal region of IPS-1, encompassing the NS3-4A recognition site and a mitochondrial targeting sequence, was fused to green fluorescent protein (EGFP-IPS, Fig. 1a) or to red fluorescent proteins (RFP), mCherry or TagRFP. An SV40 nuclear localization sequence (NLS) was included between the RFP variant and IPS-1 segment (RFP-NLS-IPS, Fig. 1a). Human hepatoma (Huh-7.5)

Correspondence should be addressed to C.M.R. (ricec@rockefeller.edu).

⁵Present address: Hepregen Corporation, 200 Boston Ave, Suite 1500, Medford, MA 02155

⁶Present address: iTherX Pharmaceuticals, P.O. Box 910530, San Diego, CA 92191-0530

Author Contributions C.T.J. and C.M.R. designed the project, analyzed results and wrote the manuscript. C.T.J., M.T.C., L.J.L., A.J.S., S.R.K., T.S.O., A.P. and J.W.S. performed the experimental work. S.R.K., J.W.S., T.S.O., M.R.M., and S.N.B. contributed reagents and technical expertise.

Competing Financial Interests The authors declare the following conflicts of interest, which are managed under University policy: C.M.R. has equity in Apath, LLC, which holds commercial licenses for the Huh-7.5 cell line and the HCVcc cell culture system. S.R.K. and S.N.B. have equity in Hepregen, Corporation, which holds commercial licenses from the Massachusetts Institute of Technology for micropatterned co-cultures (MPCCs) and other related microscale liver technologies.

cells stably transduced with lentiviruses encoding EGFP-IPS or RFP-NLS-IPS exhibited punctate fluorescence consistent with mitochondrial localization, which was confirmed by colocalization with native IPS-1 (Fig. 1b).

To determine the reporter phenotype in the presence of NS3-4A, EGFP-IPS or RFP-NLS-IPS constructs were transduced into Huh-7.5 cells stably expressing an autonomously replicating HCV subgenome⁸ (JFH-1 strain, SG-JFH). Replicon-harboring cells expressing EGFP-IPS showed diffuse fluorescence, while an NS3-4A cleavage resistant form⁹ of the reporter (EGFP-IPS(C508Y), Fig. 1c) exhibited a punctate pattern. Similarly, replicon-containing Huh-7.5 cells expressing RFP-NLS-IPS, but not RFP-NLS-IPS(C508Y), showed nuclear translocation of fluorescence (Fig. 1c). Both reporters displayed a punctate pattern in the absence of the HCV replicon (Fig. 1c). These results indicate that cleavage of EGFP-IPS and RFP-NLS-IPS are dependent on an intact NS3-4A recognition site and suggest that HCV-dependent fluorescence relocalization (HDFR) can be used as a marker of viral replication.

HCV exists as multiple genotypes, which exhibit extensive sequence divergence, as well as differences in pathogenesis and treatment susceptibility¹⁰. Evasion of the innate immune response by cleavage of native IPS-1, however, is likely to be a conserved feature of HCV infection. In addition to JFH-1 (genotype 2a), Huh-7.5 cells harboring genotype 1a (H77) or 1b (Con1) subgenomes⁸ were transduced with EGFP-IPS or EGFP-IPS(C508Y). Regardless of HCV strain, EGFP-IPS transduction resulted in diffuse fluorescence, while EGFP-IPS(C508Y) expression led to punctate EGFP (Fig. 1c). While the lack of replicon systems for other genotypes precludes comprehensive analysis, these results indicate that cleavage of EGFP-IPS can be used as a marker of several diverse HCV strains. In contrast, replication of other positive-strand RNA viruses, such as yellow fever virus (YFV) or Venezuelan equine encephalitis virus (VEE), did not lead to fluorescence relocalization (Supplemental Fig. 1a). These results suggest that the HDFR reporter system achieves a high level of HCV-specificity combined with genotype independence.

While replicon-containing cells are under selection to constitutively express the viral proteins, monitoring authentic virus infection is important for analyses of HCV biology and therapeutic inhibition. To determine the ability of HDFR to detect infection, Huh-7.5 cells expressing RFP-NLS-IPS were inoculated with an HCVcc reporter virus expressing secreted *Gaussia* luciferase, Jc1FLAG2(p7-nsGluc2A)¹¹, followed by incubation for 48 h. Uninfected cells showed punctate fluorescence, whereas HCV-infected cultures displayed a distinct nuclear signal (Fig. 1d). Inoculation in the presence of type I interferon (IFN- β) largely abolished the fluorescence translocation phenotype. Similarly, cells infected in conjunction with a monoclonal antibody targeting a known HCV entry factor (α -CD81) did not show nuclear fluorescence. Detection of *Gaussia* luciferase in the culture supernatants paralleled the appearance of nuclear RFP-NLS (Fig. 1d). Staining for viral replicase protein NS5A in infected EGFP-IPS-expressing cells supported the correspondence between fluorescence relocalization and HCV replication at the single-cell level (Supplemental Fig. 1b).

Fluorescence relocalization does not depend on signal amplification, nor does it require cells to be fixed, lysed or processed in order to detect infection. These advantages suggested the possibility of real-time visualization of HCV infection in live cells. Huh-7.5 cells expressing RFP-NLS-IPS and a constitutive mitochondrial marker (EGFP-cytochrome c oxidase subunit VIII fusion protein; mito-EGFP) were inoculated with Jc1FLAG2(p7-nsGluc2A) and monitored by live-cell microscopy beginning at 6 h post-infection (Fig. 2a and b, DMSO). Translocation of RFP-NLS to the nucleus could be detected as early as 10-12 h post-inoculation, with complete cleavage by 16-18 h, revealing infection significantly earlier

than existing methods (Fig 1b and Supplementary Video 1a). In contrast, cells infected in the presence of a viral RNA-dependent RNA polymerase inhibitor (2'CMA)¹² showed very limited nuclear fluorescence (Fig. 2b, Supplementary Video 1b). We then investigated whether drug treatment of cells with established HCV infection could lead to observable reconstitution of mitochondrially-localized fluorescence. RFP-NLS-IPS reporter cells were infected with Jc1FLAG2(p7-nsGluc2A) for 24 h before treatment with DMSO or VX-950, an inhibitor of the NS3-4A¹³ protease, and imaging for an additional 24 h (Fig. 2a, c). Over the time course of imaging, RFP-NLS-IPS localization in DMSO cells remained unchanged, while steady reconstitution of punctate fluorescence was seen in the majority of infected cells treated with the protease inhibitor. These results indicate that the reporter system can be used to visually monitor NS3-4A inhibition in real time (Supplementary Videos 1c and d).

The availability of spectrally distinct HDFR reporters (EGFP-IPS and RFP-NLS-IPS) suggested the possibility of discerning infection in two separate cell populations simultaneously. We applied this advantage to visualize the recently described phenomenon of CD81-independent HCV infection. Circulating HCV enters hepatocytes through a complex pathway involving multiple co-receptors. CD81, SR-B1, and two tight-junction proteins, CLDN1 and OCLN, have been shown to be essential for this process¹⁴⁻¹⁷. Recent reports, however, suggest a second, CD81-independent route of virus entry, which may entail particle transfer through close cell-cell contacts^{18, 19}. This transmission mode may be highly biologically relevant in the context of chronic infection, and the development of inhibitors targeting this entry pathway necessitates a reliable method of detection. To monitor routes of HCV spread, we employed RFP-NLS-IPS and EGFP-IPS transduced cells as producer and target populations, respectively. EGFP-IPS target cells were engineered to stably express an shRNA targeting CD81 (EGFP-IPS/CD81⁻) or an irrelevant sequence (EGFP-IPS/IRR), and tested for permissiveness to cell-free virus using an adapted HCVcc (J6/JFH clone 2), which exhibits superior titers to J6/JFH (*Diamond, D. L. et al PLoS Pathog. in press*). At 48 h post-infection, the majority of EGFP-IPS/IRR cells exhibited diffuse EGFP, while EGFP-IPS/CD81⁻ cells were largely non-permissive (Fig. 3a). FACS analysis of fixed samples stained with an NS5A antibody supported these observations, indicating that less than 1% of EGFP-IPS/CD81⁻ cells were infected, compared to ~80% of the EGFP-IPS/IRR targets (Supplementary Fig. 2). To investigate HCV transmission in a mixed cell population, RFP-NLS-IPS cells were pre-infected for 36 h before co-culturing with EGFP-IPS/IRR or EGFP-IPS/CD81⁻ target cells. Mixing uninfected RFP-NLS-IPS cells with either target population did not result in EGFP relocalization. In contrast, the majority of EGFP-IPS/IRR cells exhibited diffuse fluorescence upon co-culture with infected producers, presumably as a result of both CD81-dependent and -independent infection routes. Culture of infected producer cells with EGFP-IPS/CD81⁻ targets also led to EGFP-IPS cleavage, correlating with CD81-independent infection of 10-15% of cells (Fig. 3a and Supplementary Fig. 2). Use of the HDFR system in a mixed population can therefore provide a rapid visual assay for CD81-independent HCV spread.

In addition to exploiting a number of cellular factors during virus uptake, HCV impacts host pathways during replication and pathogenesis. The ability to correlate infection with altered cell biology on a single-cell level would be invaluable to detecting virus-induced phenotypes. We therefore examined whether HDFR could be multiplexed with fluorescent markers of host processes. Stress pathways are charged with protecting the cell against various environmental insults, including heat shock, oxidative stress, and virus infection. In response to stress, phosphorylation of translation factor eIF2 α leads to the appearance of cytoplasmic stress granules, in which mRNAs are triaged and translation is stalled (reviewed in²⁰). Not surprisingly, many viruses have evolved mechanisms to modulate the stress response and subvert translational suppression (reviewed in²¹); the effect of HCV on stress

granule formation is unknown. We examined stress response in Huh-7 cells expressing RFP-NLS-IPS and EGFP-tagged Ras-Gap-SH3 domain binding protein (EGFP-G3BP), a marker of stress granule formation²². Transduced cells were infected with Jc1FLAG2(p7-nsGluc2A) and subsequently monitored by live cell imaging; HCV replication was readily observed starting at 14-16 h post-infection. EGFP-G3BP exhibited a cytoplasmic distribution until approximately 30 h post-infection, when stress granule formation commenced in a fraction of HCV-positive cells. Interestingly, stress granules often appeared to be transient and, in some cases, formed and dissolved multiple times within a single cell (Fig. 3b). Stress granule formation was not observed in neighboring uninfected cells, nor in infected cultures treated with 2'CMA (Supplementary Videos 2a-c), suggesting a dependence on HCV replication. While the mechanisms underlying this phenomenon are still obscure, these observations support the power of single-cell analysis and reporter multiplexing for discovery and dissection of virus-host interactions.

While we have demonstrated that fluorescence relocalization can be used to detect infection of highly permissive hepatoma cell lines, we sought to monitor HCV uptake by primary human hepatocytes. Primary cells are arguably the most relevant culture system in which to study HCV biology, but have traditionally been subject to substantial challenges. Primary hepatocytes show low permissiveness for both viral entry and RNA replication, leading to poor expression of HCV-specific antigens, and making standard immunofluorescence techniques unreliable for visualizing infection. We reasoned that the sensitivity of HDFR might circumvent these difficulties, and explored its use for detecting HCV infection in the recently developed micropattern co-culture (MPCC) system²³. MPCCs consist of primary adult human hepatocytes seeded on islands of collagen and surrounded by mouse fibroblast "feeder" cells. These conditions allow hepatocytes to be maintained for extended periods without the rapid decline in cellular functions seen in conventional monocultures or random co-cultures²⁴. To visualize HCV infection in MPCC hepatocytes, cultures were transduced with RFP-NLS-IPS or RFP-NLS-IPS(C508Y), followed 48 h later by infection with Jc1FLAG2(p7-nsGluc2A), allowing MPCC infection to be monitored in parallel by *Gussia* luciferase secretion (Supplementary Fig. 3). MPCC islands were examined by live cell microscopy and the cells per island exhibiting nuclear RFP were enumerated (Fig. 3c). In cultures transduced with RFP-NLS-IPS followed by DMSO treatment, approximately 98% of the islands observed contained cells with nuclear RFP, averaging 4 cells/island. In the RFP-NLS-IPS population treated with 2'CMA, only 6% of islands exhibited infected cells, corresponding to an average of 0.06 cells/island. Cells transduced with RFP-NLS-IPS(C508Y) did not show nuclear RFP in any of the islands examined (Fig. 3c). These results indicate that infection of primary hepatocytes can be readily detected using the HDFR system. Importantly, this represents the first method capable of visualizing HCV infection in live primary hepatocytes.

Although systems for tracking HCV replication in culture have expanded rapidly in recent years, robust detection methods applicable to imaging of individual live cells have not been available. We describe a sensitive HCV reporter that allows easy distinction of infected and uninfected cells in live or fixed cultures by standard fluorescence microscopy. The robust signal of the reporter system derives from the efficiency of NS3-4A cleavage and the constitutive high-level expression of the substrate; nuclear translocation increases visualization, as the reporter becomes concentrated in a region with low autofluorescence, a particular advantage when working with hepatocytes. While reporter cleavage does not occur in the absence of an active protease, transient signal may be expected in the presence of a polymerase inhibitor – this high sensitivity may have to be factored in as "background" for some applications. The HDFR system does not require genetic modification of the viral genome and showed efficient detection of all HCV genotypes tested. This raises the possibility of using the reporter to identify novel infectious isolates directly from patient

samples, potentially expanding the HCVcc system beyond the currently available genotype 2a strain. Coaxing HCVcc to infect biologically relevant primary cell types may also be key to understanding authentic viral processes and patient-specific responses. The low level of replication observed in these cultures may reflect heterogeneity between individual cells or viral genomes, and underscores the value of single-cell analysis in dissecting the often subtle or variable phenotypes associated with chronic infection. Combining HDFR-based visualization with laser capture microscopy and analysis of neighboring infected and uninfected cells could begin to unravel the determinants of pathogenesis or virus control. The value of single-cell analysis was further illustrated by multiplexing HCV detection with a fluorescent marker of cellular stress, allowing direct visual correlation of viral and host events. Recent advances in automated microscopy and “high-content” screening have made a large number of cellular phenotypes, including drug toxicity profiles, accessible to interrogation in a multiparametric format (reviewed in ²⁵). Addition a robust fluorescent translocation assay requiring minimal sample processing has the potential to integrate HCV research into this burgeoning field. We anticipate that the ability of HDFR to increase the flexibility and diversity of HCV culture systems will be an important step towards creating new platforms for basic virology and antiviral drug development.

Methods

Cell culture

Huh-7 and Huh-7.5 cells were cultured at 37°C, 5% CO₂ in Dulbecco’s Modified Eagle Medium (DMEM, Invitrogen) containing 10% fetal bovine serum (FBS) and 0.1 mM nonessential amino acids (NEAA) (complete media), unless otherwise noted. For time-lapse imaging, cells were maintained in CO₂-independent media (Invitrogen) containing 10% FBS, 0.1 mM NEAA, 1 mM sodium pyruvate and 2 mM L-glutamine (imaging media). Huh-7.5 cell lines harboring selectable subgenomic replicons⁸ were grown in complete media containing 0.5 mg/ml G418. Huh-7.5 cells stably expressing the pLenti-3’-U6-EC-EP7 vector encoding an shRNA against CD81 (nt 268-288, cDNA numbering) or a predicted non-targeting sequence (IRR) have been previously described¹⁹ and were grown in complete media containing 6 µg/ml blasticidin. MPCC cultures were generated as previously described²³ and maintained in high glucose DMEM, 10% FBS, 0.5 U/ml insulin, 7 ng/ml glucagon, 7.5 µg/ml hydrocortisone and 1% penicillin-streptomycin. For HCV inhibition, culture media was supplemented with 0.2% DMSO, 14 mM 2’CMA, 24 mM VX-950, or 1000 U/ml IFN-β (Peprotech). For neutralization experiments, HCVcc infections were performed in the presence 10 µg/ml antibody directed against CD81 (BD Biosciences) or an isotype control (IgG1κ, BD Biosciences).

Virus stocks

Jc1²⁶ and Jc1FLAG2(p7-nsGluc2A)¹¹ are fully-infectious HCVcc viruses that have been previously described. J6/JFH clone 2 is a passaged derivative of J6/JFH²⁷ that contains a number of adaptive mutations that increase infectious titers (*Diamond D. L. et al, PLoS Pathogens, in press*). Bi-Ypet-Jc1FLAG2 is a bicistronic reporter virus in which the HCV IRES drives expression of Ypet, an EGFP variant with enhanced brightness, in the first cistron; the EMCV IRES drives expression of the second cistron, which encodes the Jc1 polyprotein with a FLAG epitope at the N-terminus of E2. YF17D(5’C25Venus2AUbi) is a monocistronic yellow fever reporter virus (kindly provided by C. Stoyanov, The Rockefeller University) encoding the Venus fluorescent protein, a yellow-shifted variant of EGFP. VEE-EGFP (kindly provided by I. Frolov, UTMB) is a double subgenomic EGFP reporter virus derived from the TC83 vaccine strain of Venezuelan equine encephalitis. Virus stocks were generated by electroporation of in vitro transcribed RNAs into the appropriate cell lines, as described previously²⁷⁻²⁹.

Plasmid constructs

Constructs were created by standard methods; plasmid and primer sequences are available upon request. IPS-1 based reporters and subcellular localization markers were constructed in a lentivirus backbone derived from TRIP-EGFP³⁰. Residues 462 to 540 of IPS-1 (IPS) were obtained by PCR from a human hepatocyte cDNA library (Ambion) and inserted into the BsrGI/XhoI sites of TRIP-EGFP to generate TRIP-EGFP-IPS. IPS-1 mutation C508Y was generated by overlap PCR mutagenesis. TRIP-mCherry and TRIP-TagRFP were used to construct TRIP-RFP-NLS-IPS plasmids. TRIP-mCherry was derived from the TRIP-mCherry-CLDN1 plasmid¹⁶. TagRFP sequence was obtained from pTagRFP-C (Evrogen). TRIP-RFP-NLS-IPS plasmids encode the SV40 nuclear localization signal (NLS, PKKKRKVVG) and IPS fused to the C-terminus of RFP. TRIP-mito-EGFP, encodes the mitochondrial targeting sequence of human cytochrome c oxidase subunit VIIIa fused to the N-terminus of EGFP. TRIP-EGFP-G3BP encodes the Ras-Gap-SH3 domain binding protein (G3BP, kindly provided by J. Tazi²²) fused to the C-terminus of EGFP.

Generation of lentivirus pseudoparticles and transductions

Pseudoparticles (pp) were generated by co-transfection of 293T cells with TRIP provirus, HIV gag-pol, and vesicular stomatitis virus envelope protein G (VSV-G) plasmids using a weight ratio of 1:0.8:0.2, as described previously¹⁶. Huh-7 and Huh-7.5 cells were transduced by incubation for 6 h at 37°C with TRIPpp diluted 1:3 in complete media supplemented with 4 µg/ml polybrene and 20 mM HEPES. In some cases, transduced hepatoma cell populations were enriched using a FACSaria II high-speed flow cytometry cell sorter (BD Biosciences). For transduction of MPCC, cultures were first treated for ~20 sec with 0.025% EDTA/Trypsin, before washing and overnight incubation with 1:3 diluted TRIPpp stocks.

Immunofluorescence staining and FACS analysis

For NS5A immunostaining, cells grown on glass coverslips were washed with phosphate-buffered saline (PBS) prior to fixation in formaldehyde (3.7% w/v in PBS) and incubation in blocking buffer (3% BSA, 0.2% saponin in PBS). After overnight incubation at 4°C with monoclonal antibody 9E10²⁷ (1:2000 in blocking buffer) and 1 h incubation at RT with AlexaFluor-594-conjugated secondary antibody to mouse (Invitrogen, 1:1000 in blocking buffer), cell nuclei were stained with Hoechst dye (Thermo scientific). Coverslips were mounted using ProLong Gold Antifade reagent (Invitrogen). For IPS-1 immunostaining, cells grown on glass bottom multiwell plates (MatriCal) were washed with PBS and fixed with 2% paraformaldehyde. After incubation in blocking buffer for 30 min, and polyclonal anti-IPS-1 antibody (Cell Signaling Technology) for 2 h, AlexaFluor-555 or AlexaFluor-488 conjugated anti-rabbit IgG secondary antibodies (Cell Signaling Technology) were added for 1 h at RT. Cells were then stained with Hoechst nuclear dye followed by application of ProLong Gold Antifade reagent. For FACS analysis, cells were harvested using AccuMax (eBioscience) and fixed using Fixation/Permeabilization buffer (BD Biosciences) for 10 min at 4°C. Fixed cells were washed with BD Perm/Wash buffer (BD Biosciences), incubated 30 min at RT with AlexaFluor-647-conjugated 9E10 antibody (1:4000 in BD Perm/Wash buffer), washed twice with BD Perm/Wash buffer and once with FACS buffer (PBS/3%FBS) prior to analysis using a BD LSR II flow cytometer and BD FACSDiva software. Analysis of was performed using FlowJo software.

Microscopy

Wide-field fluorescent images were captured using an Eclipse TE300 (Nikon) inverted microscope and SPOT imaging software or the Discovery-1 system and MetaXpress software (Molecular Devices). Confocal imaging of fixed samples was performed using an

inverted Axiovert 200 laser scanning microscope (Zeiss). For long-term live cell imaging, cells were grown on rat-tail collagen coated (BD Biosciences) no. 1.5 Lab-Tek II 4-chambered (Thermo Fisher Scientific) coverslips. Live cells maintained at 37°C in imaging media were imaged using a Zeiss Axiovert 200 inverted microscope equipped with an UltraView spinning disk confocal head (Perkin-Elmer), an Orca ER cooled CCD camera (Hamamatsu), a 20×/0.75 N.A. Plan-Apochromat objective, and an environmental chamber (Solent Scientific). Solid state 491 and 561 nm lasers (Spectral Applied) and ET 530/50 and ET 605/70 emission filters (Chroma) were used for excitation and emission of EGFP and RFP fluorescence, respectively. Alternatively, time lapse images were captured using an Olympus IX71 inverted microscope equipped with an Orca ER cooled CCD camera, a 20×/0.75 N.A. UPlan SApo objective and an environmental chamber. Image acquisition was performed using Metamorph (Molecular Devices) and processing was performed using ImageJ64.

Supplementary Material

Refer to Web version on PubMed Central for supplementary material.

Acknowledgments

We acknowledge the expert support of The Rockefeller University Bioimaging Core Facility, with special thanks to A. North, S. Galdeen and S. Bhuvanendran. We thank The Rockefeller University Flow Cytometry Resource Center, supported by the Empire State Stem Cell Fund through NYSDOH Contract #C023046; opinions expressed here are solely those of the authors and do not necessarily reflect those of the Empire State Stem Cell Fund, the NYSDOH, or the State of NY. We are grateful to C. Stoyanov, J. Tazi (Institut de Genetique Moleculaire de Montpellier) and I. Frolov (UTMB) for contribution of reagents. We thank M. Holz, A. Forest, M. Panis, and A. Webson for laboratory support and C. Murray for critical reading of the manuscript. This work was supported by PHS grant R01 AI075099, Greenberg Medical Research Institute, and the Starr Foundation. C.T.J. was supported by a National Research Service Award DK081193; M.T.C. by a Women & Science Fellowship; L.J.L. is supported by a Natural Sciences and Engineering Research Council of Canada fellowship. A.P. is a recipient of a Kimberly Lawrence-Netter cancer research discovery fund award.

References

1. Shepard CW, Finelli L, Alter MJ. Global epidemiology of hepatitis C virus infection. *Lancet Infect Dis.* 2005; 5:558–567. [PubMed: 16122679]
2. Meylan E, et al. Cardif is an adaptor protein in the RIG-I antiviral pathway and is targeted by hepatitis C virus. *Nature.* 2005; 437:1167–1172. [PubMed: 16177806]
3. Foy E, et al. Control of antiviral defenses through hepatitis C virus disruption of retinoic acid-inducible gene-1 signaling. *Proc Natl Acad Sci U S A.* 2005; 102:2986–2991. [PubMed: 15710892]
4. Li XD, Sun L, Seth RB, Pineda G, Chen ZJ. Hepatitis C virus protease NS3/4A cleaves mitochondrial antiviral signaling protein off the mitochondria to evade innate immunity. *Proc Natl Acad Sci U S A.* 2005; 102:17717–17722. [PubMed: 16301520]
5. Kawai T, et al. IPS-1, an adaptor triggering RIG-I- and Mda5-mediated type I interferon induction. *Nat Immunol.* 2005; 6:981–988. [PubMed: 16127453]
6. Seth RB, Sun L, Ea CK, Chen ZJ. Identification and characterization of MAVS, a mitochondrial antiviral signaling protein that activates NF- κ B and IRF 3. *Cell.* 2005; 122:669–682. [PubMed: 16125763]
7. Xu LG, et al. VISA is an adapter protein required for virus-triggered IFN- β signaling. *Mol Cell.* 2005; 19:727–740. [PubMed: 16153868]
8. Tscherne DM, et al. Superinfection exclusion in cells infected with hepatitis C virus. *J Virol.* 2007; 81:3693–3703. [PubMed: 17287280]
9. Loo YM, et al. Viral and therapeutic control of IFN- β promoter stimulator 1 during hepatitis C virus infection. *Proc Natl Acad Sci U S A.* 2006; 103:6001–6006. [PubMed: 16585524]

10. Simmonds P. Genetic diversity and evolution of hepatitis C virus-15 years on. *J Gen Virol.* 2004; 85:3173–3188. [PubMed: 15483230]
11. Marukian S, et al. Cell culture-produced hepatitis C virus does not infect peripheral blood mononuclear cells. *Hepatology.* 2008; 48:1843–1850. [PubMed: 19003912]
12. Carroll SS, et al. Inhibition of hepatitis C virus RNA replication by 2'-modified nucleoside analogs. *J Biol Chem.* 2003; 278:11979–11984. [PubMed: 12554735]
13. Lin K, Perni RB, Kwong AD, Lin C. VX-950, a novel hepatitis C virus (HCV) NS3-4A protease inhibitor, exhibits potent antiviral activities in HCV replicon cells. *Antimicrob Agents Chemother.* 2006; 50:1813–1822. [PubMed: 16641454]
14. Pileri P, et al. Binding of hepatitis C virus to CD81. *Science (New York, NY).* 1998; 282:938–941.
15. Scarselli E, et al. The human scavenger receptor class B type I is a novel candidate receptor for the hepatitis C virus. *EMBO Journal.* 2002; 21:5017–5025. [PubMed: 12356718]
16. Evans MJ, et al. Claudin-1 is a hepatitis C virus co-receptor required for a late step in entry. *Nature.* 2007; 446:801–805. [PubMed: 17325668]
17. Ploss A, et al. Human occludin is a hepatitis C virus entry factor required for infection of mouse cells. *Nature.* 2009; 457:882–886. [PubMed: 19182773]
18. Timpe JM, et al. Hepatitis C virus cell-cell transmission in hepatoma cells in the presence of neutralizing antibodies. *Hepatology.* 2008; 47:17–24. [PubMed: 17941058]
19. Witteveldt J, et al. CD81 is dispensable for hepatitis C virus cell-to-cell transmission in hepatoma cells. *J Gen Virol.* 2009; 90:48–58. [PubMed: 19088272]
20. Anderson P, Kedersha N. RNA granules. *J Cell Biol.* 2006; 172:803–808. [PubMed: 16520386]
21. Schutz S, Sarnow P. How viruses avoid stress. *Cell Host Microbe.* 2007; 2:284–285. [PubMed: 18005747]
22. Tourriere H, et al. The RasGAP-associated endoribonuclease G3BP assembles stress granules. *J Cell Biol.* 2003; 160:823–831. [PubMed: 12642610]
23. Khetani SR, Bhatia SN. Microscale culture of human liver cells for drug development. *Nat Biotechnol.* 2008; 26:120–126. [PubMed: 18026090]
24. Bhatia SN, Balis UJ, Yarmush ML, Toner M. Effect of cell-cell interactions in preservation of cellular phenotype: cocultivation of hepatocytes and nonparenchymal cells. *FASEB J.* 1999; 13:1883–1900. [PubMed: 10544172]
25. Wollman R, Stuurman N. High throughput microscopy: from raw images to discoveries. *J Cell Sci.* 2007; 120:3715–3722. [PubMed: 17959627]
26. Pietschmann T, et al. Construction and characterization of infectious intragenotypic and intergenotypic hepatitis C virus chimeras. *Proc Natl Acad Sci U S A.* 2006; 103:7408–7413. [PubMed: 16651538]
27. Lindenbach BD, et al. Complete replication of hepatitis C virus in cell culture. *Science.* 2005; 309:623–626. [PubMed: 15947137]
28. Lindenbach BD, Rice CM. Trans-complementation of yellow fever virus NS1 reveals a role in early RNA replication. *Journal of virology.* 1997; 71:9608–9617. [PubMed: 9371625]
29. Petrakova O, et al. Noncytopathic replication of Venezuelan equine encephalitis virus and eastern equine encephalitis virus replicons in mammalian cells. *J Virol.* 2005; 79:7597–7608. [PubMed: 15919912]
30. Zennou V, et al. HIV-1 genome nuclear import is mediated by a central DNA flap. *Cell.* 2000; 101:173–185. [PubMed: 10786833]

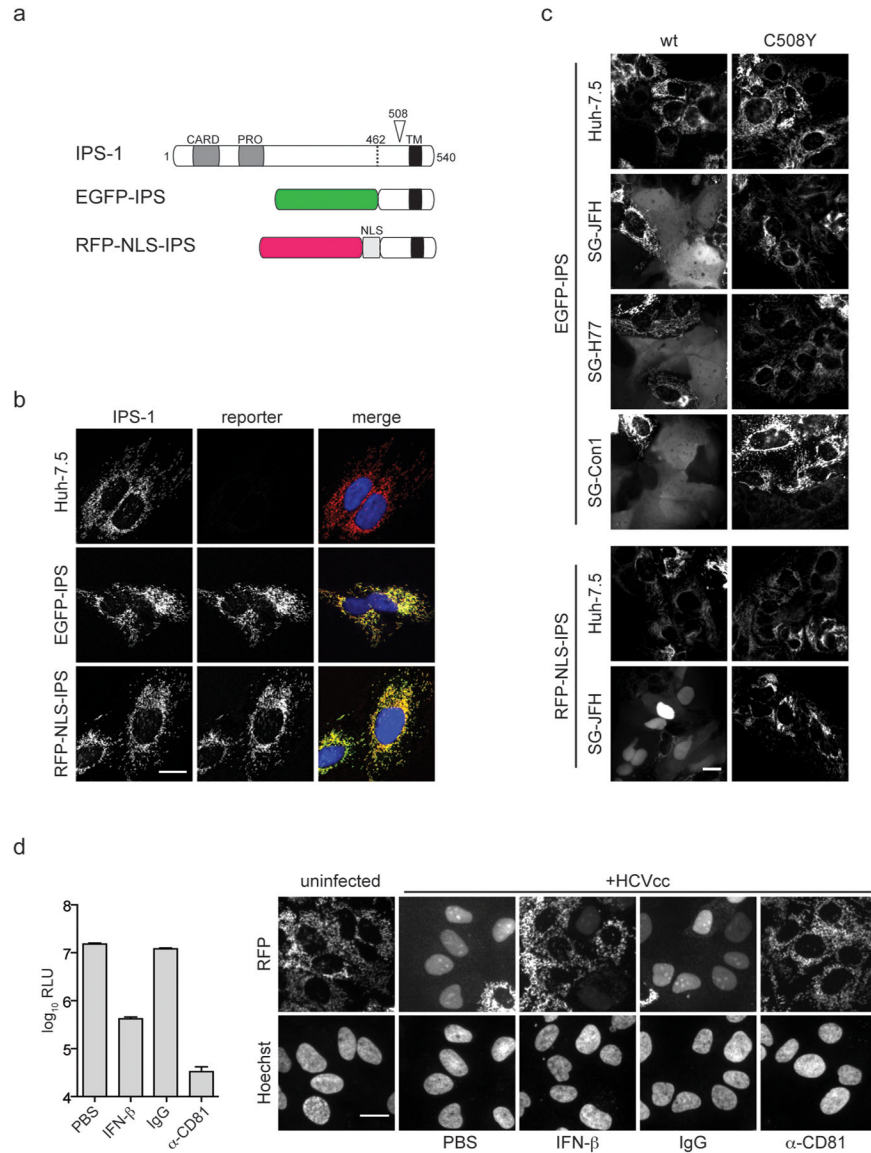


Figure 1. An IPS-1-based reporter system for detection of HCV infection

(a) Schematic of IPS-1 and derivative reporter constructs. The Caspase Recruitment Domain (CARD) and proline rich (PRO) domains of IPS-1, also known as MAVS⁶, VISA⁷, or Cardif², are indicated. The HCV NS3-4A protease cleaves IPS-1 at C508 (arrow). The C-terminal transmembrane domain (TM) directs IPS-1 to the outer membrane of mitochondria. EGFP-IPS encodes EGFP fused to residues 462-540 of IPS-1. RFP-NLS-IPS encodes a red fluorescent protein (mCherry or TagRFP) and an SV40 nuclear localization signal (NLS, PKKKRKVG) fused to residues 462-540 of IPS-1. **(b)** EGFP-IPS and RFP-NLS-IPS localize to mitochondria in Huh-7.5 cells. Native IPS-1, detected by immunofluorescent staining (IPS-1), as well as EGFP or RFP autofluorescence (reporter) were visualized in untransduced (Huh-7.5) or transduced (EGFP-IPS or RFP-NLS-IPS) cells by confocal microscopy. Merge images also depict Hoechst nuclear dye (blue). **(c)** EGFP-IPS and RFP-NLS-IPS relocate in response to HCV replication. Huh-7.5 cell lines harboring subgenomic (SG) neomycin-selectable replicons were transduced with lentiviruses expressing wild type (wt) or mutant (C508Y) EGFP-IPS or RFP-NLS-IPS. H77, genotype

1a; Con1, genotype 1b; JFH-1, genotype 2a. Wide-field fluorescence images of unfixed cells are shown. **(d)** RFP-NLS-IPS relocalizes in HCV infected cells. Huh-7.5 cells expressing RFP-NLS-IPS were infected with secreted *Gaussia* luciferase HCVcc reporter virus, Jc1FLAG2(p7-nsGluc2A), in the presence of phosphate buffered saline (PBS), IFN- β , blocking antibody (α -CD81) or isotype control (IgG). Luciferase activity in the culture supernatants (left) and reporter (RFP) or nuclear dye (Hoechst) fluorescence (right) were monitored at 48 h post-infection. Wide-field fluorescence images of fixed cells are shown. Scale bars, 20 μ m. RLU, relative light units.

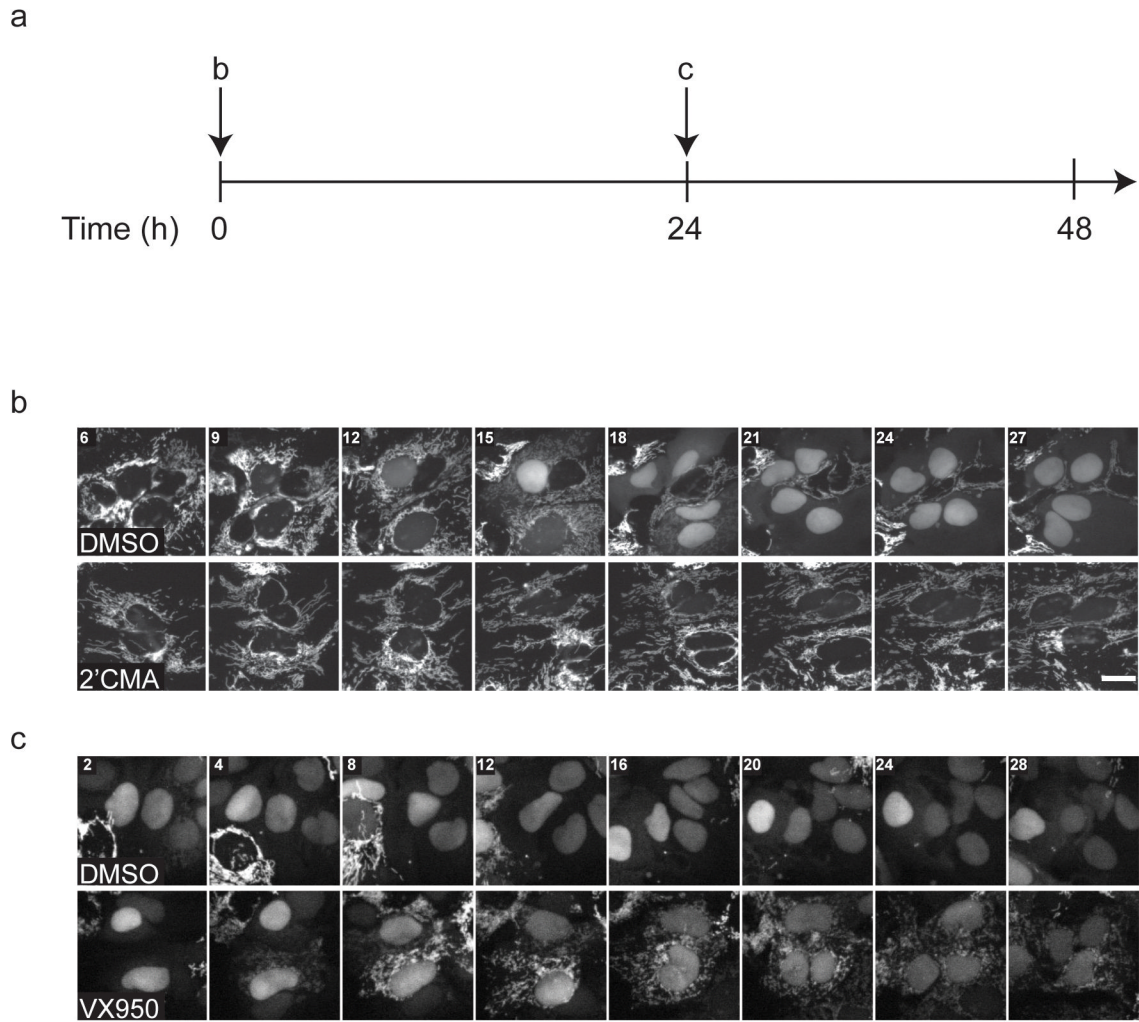


Figure 2. Time-lapse live-cell imaging of HCVcc infection

(a) Schematic of live-cell imaging time course. Huh-7.5 cells stably expressing RFP-NLS-IPS and a mitochondrially targeted EGFP-cytochrome c oxidase subunit VIII fusion protein (mito-EGFP) were infected with HCVcc reporter virus, Jc1FLAG2(p7-nsGluc2A). (b) Cells were infected in the presence of DMSO or HCV RNA-dependent RNA polymerase inhibitor 2'CMA. (c) Cells were infected for 24 h prior to removal of the inoculum and addition of imaging medium containing DMSO or the NS3-4A protease inhibitor VX950. Images were captured every 30 min starting at 6 h (b) or 24.5 h (c) post-infection. RFP fluorescence is shown in grayscale. Time (h) from the start of infection (b) or drug addition (c) are indicated. Scale bar, 20 μ m. See Supplementary Videos 1a-d for full time course.

co-cultures (MPCC) were transduced with lentiviruses expressing wild type (wt) or mutant (C508Y) RFP-NLS-IPS. At 24 h post-transduction, MPCC were infected with Jc1FLAG2(p7-nsGluc2A). After 12 h, virus was removed and MPCC medium containing DMSO or 2'CMA was added. Unfixed MPCCs were imaged by wide-field fluorescence microscopy at 48 h post-infection. Representative phase contrast (top row) and corresponding RFP fluorescence images (middle row) are shown. Enlarged fluorescence images (bottom row) correspond to area denoted by white dotted box (middle row). The number of cells per MPCC island exhibiting nuclear RFP at 48 h post-infection is plotted for each condition. For wt RFP-NLS-IPS+DMSO n=40; wt RFP-NLS-IPS+2'CMA n=30; C508Y RFP-NLS-IPS+DMSO n=35. Bar, mean number of positive cells/island. Scale bars, 20 μm (a and b), 200 μm (c, top panel), 10 μm (c, lower panel).